Destruction of islands of stability

1999 J. Phys. A: Math. Gen. 32 5213

(http://iopscience.iop.org/0305-4470/32/28/303)

J. Phys. A: Math. Gen. **32** (1999) 5213–5232. Printed in the UK PII: S0305-4470(99)00925-7

Destruction of islands of stability

G Contopoulos†‡, M Harsoula‡, N Voglis‡ and R Dvorak§

† Research Center for Astronomy, Academy of Athens, Greece
‡ Astronomy Department, University of Athens, Greece
§ Institute for Astronomy, University of Vienna, Austria

Received 14 January 1999

Abstract. We describe the changes and the destruction of islands of stability in four dynamical systems: (a) the standard map, (b) a Hamiltonian with a cubic nonlinearity, (c) a Hamiltonian with a quartic nonlinearity and (d) the Sitnikov problem. As the perturbation increases the size of the island increases and then decreases abruptly. This decrease is due to the joining of an outer and an inner chaotic domain. The island disappears after a direct (supercritical) or an inverse (subcritical) bifurcation of its central periodic orbit C. In the first case, when C becomes unstable, a chaotic domain is formed near C. This domain is initially separated from the outer 'chaotic sea' by KAM curves. But as the perturbation increases the inner chaotic domain grows outwards, while the outer 'chaotic sea' progresses inwards. The last KAM curve is destroyed by forming a cantorus and the two chaotic domains join. But even then the escape of orbits through the cantorus takes a long time (stickiness effect). In the inverse bifurcation case the island around the central orbit is limited by two equal period unstable orbits. As the perturbation changes these two orbits approach and join the central orbit, that becomes unstable. Then the island disappears but no cantori are formed. In this case the stickiness is due to the delay of deviation of an orbit from the unstable periodic orbit when its eigenvalue is not much larger than 1.

1. Introduction

Islands of stability appear generically in conservative dynamical systems. Even when chaos is dominant, in most cases there are stable periodic orbits surrounded by small islands of stability. As an example we consider islands of stability in the well known standard map

$$\left.\begin{aligned} x_{i+1} &= x_i + y_{i+1} \\ y_{i+1} &= y_i + \frac{K}{2\pi}\sin(2\pi x_i) \end{aligned}\right\} \quad (\mathrm{mod}\ 1) \tag{1}$$

where K is the nonlinearity parameter (section 2). We will also discuss briefly the islands of stability on a Poincaré surface of a section of the Hamiltonians:

$$H \equiv \tfrac{1}{2}(\dot{x}^2 + \dot{y}^2 + \omega_1^2 x^2 + \omega_2^2 y^2) - \epsilon x y^2 = h \tag{2}$$

and

$$H \equiv \tfrac{1}{2}(\dot{x}^2 + \dot{y}^2 + x^2 + y^2) + \epsilon x^2 y^2 = h \tag{3}$$

for fixed energy and varying nonlinearity ϵ (sections 3 and 4), and in the Sitnikov problem for varying eccentricity e of the primaries (section 5).

The problem is how the islands of stability that exist for a given nonlinearity parameter are destroyed as K, ϵ or e, changes.

We will see that there are two main mechanisms for the destruction of the islands of stability.

0305-4470/99/285213+20$30.00

(1) The stable periodic orbit at the centre of the island becomes unstable, by an equal period or a period doubling bifurcation. Then a chaotic domain is produced around it, which increases outwards. Finally, the large chaotic sea outside the island and the inner chaotic domain at the centre merge and the island is destroyed.
(2) The island is limited on the outside by two equal or double period unstable periodic orbits that come closer and closer to the centre of the island. These unstable periodic orbits are followed by chaotic domains. When they merge, the stable periodic orbit at the centre of the island becomes unstable, and the outer chaotic domains join into a large chaotic sea.

These two cases correspond to direct and inverse pitchfork bifurcations, respectively (Contopoulos 1983a). The two types of bifurcations correspond to supercritical and subcritical pitchfork bifurcations, respectively (Argyris *et al* 1994). In the first case the bifurcating family (of equal or double period) is stable, and appears on the side where the original family is unstable. In the second case the bifurcating family is unstable and appears on the side where the original family is stable. In this paper we consider examples of type (1) when the stable orbits become unstable by increasing the perturbation, and examples of type (2) when the stable orbits become unstable by decreasing the perturbation.

A detailed theoretical exploration of the various types of bifurcations is provided by Hénon (1965) and by Contopoulos (1970, 1983b).

2. The evolution of the main island in the standard map

It is well known that the standard map for K larger than a critical value $K_{crit} = 0.97$ does not have invariant curves extending all the way from $x = 0$ to $x = 1$. For larger K, but smaller than $K_{cc} = 4$ there is a major island around the stable periodic orbit ($x = 0.5$, $y = 0$). This island is split into two for K larger than K_{cc}.

In this paper we will follow the evolution of one of these two islands for $K \geqslant 4.75$ until it is destroyed for K at about 6.34.

We call this island the 'main island'.

The structure of an island is well known. It consists of invariant curves surrounding a stable periodic orbit and a hierarchy of secondary islands. For example, figure 1 gives the main island for $K = 4.75$. The most important secondary islands are those with rotation number

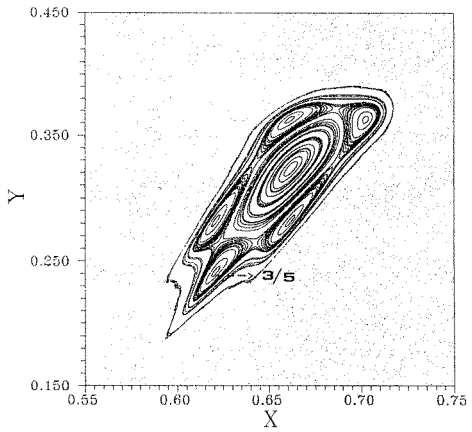

Figure 1. The main island for $K = 4.75$. We see inside the last KAM secondary islands corresponding to the resonance 3/5.

3/5. These are surrounding a stable periodic orbit of type 3/5, i.e. consisting of five stable points, say 1 2 3 4 5, visited in the sequence 1 4 2 5 3 1... clockwise. (If we consider the successive points counterclockwise the same orbit is called type 2/5. For consistency with the other types of orbits we adopt here the rotation is clockwise).

Between the five islands there is an unstable periodic orbit, also of type 3/5. There are many more chains of islands that are not marked in figure 1, as well as islands of higher order around the five islands, forming a hierarchical structure.

The island is limited by a 'last KAM curve' and beyond it there is a large 'chaotic sea', i.e. a large connected chaotic domain.

Inside the last KAM curve there are small domains of chaos around each unstable periodic orbit, but these chaotic domains do not communicate with the outer 'chaotic sea'.

However, as K increases, the last KAM curve is destroyed, i.e. it becomes a cantorus (Aubry 1978, Percival 1979) with infinite gaps, allowing the communication of the inner chaotic domains with the outer 'chaotic sea'. Thus the size of the island decreases abruptly at a critical value $K = K_c$. But for K slightly above the critical value K_c the communication through the cantorus takes a long time. During that time orbits starting inside the cantorus are stuck inside it and only later escape to the outer chaotic sea. The phenomenon of stickiness was observed first by Contopoulos (1971) and given that name by Shirts and Reinhardt (1982).

The crossing of a cantorus is usually considered by calculating orbits in the standard map, starting inside the cantorus, until one point is outside the cantorus. Then one can calculate the diffusion through the cantorus (Chirikov and Shepelyansky 1984, Dana and Fishman 1985, Meiss and Ott 1986). A more detailed way to see the crossing of a cantorus is by calculating an unstable asymptotic curve from an unstable periodic orbit, close, but inside the cantorus, until this curve crosses a gap of the cantorus (Efthymiopoulos *et al* 1997). Actually, such an asymptotic curve crosses the cantorus many times outwards and inwards before going far away from the cantorus into the large 'chaotic sea'.

The size of an island can be found if we know the last KAM curve around it. A method to find accurately the KAM curves in an island of stability has been developed by Voglis and Efthymiopoulos (1998) and by Voglis *et al* (1998). This method is based on the calculation of the rotation angles, θ, around the centre of the island, and of the 'twist angles', ϕ, between the deviations ξ_i and ξ_{i+1} from successive iterates of the map. The average values of θ and ϕ give two frequencies ν_θ and ν_ϕ.

If an orbit forms a closed invariant curve around the centre of the island, the two frequencies are equal

$$\nu_\theta = \nu_\phi. \tag{4}$$

In the case of a secondary island the value of ν_θ is constant, while ν_ϕ varies smoothly taking locally a U-form or an inverse U-form. The local minimum or maximum corresponds to the centre of the secondary island. The difference $\nu_\kappa = \nu_\phi - \nu_\theta$ is the 'epicyclic frequency' of the secondary island.

In the case of chaotic orbits the difference between the twist and rotation frequencies $\nu_\phi - \nu_\theta$ varies wildly.

The accuracy of determining ν_κ is of order $O(1/N)$. In the case of KAM curves that close around the centre of the island $\nu_\kappa = 0 + \delta/N$, where $0 < \delta < 1$ (1 means a complete cycle). Thus the quantity $R = [N\nu_\kappa]$ (the integer part of the product of the number of iteration times the epicyclic frequency) is exactly zero on such KAM curves while it tends to infinity in all ather cases, i.e. in higher order islands or in chaotic orbits. The index R is called ROTOR (ROtational TOri Recognizer). The size of an island is determined by the last point along an axis from the centre of the island, at which R is zero.

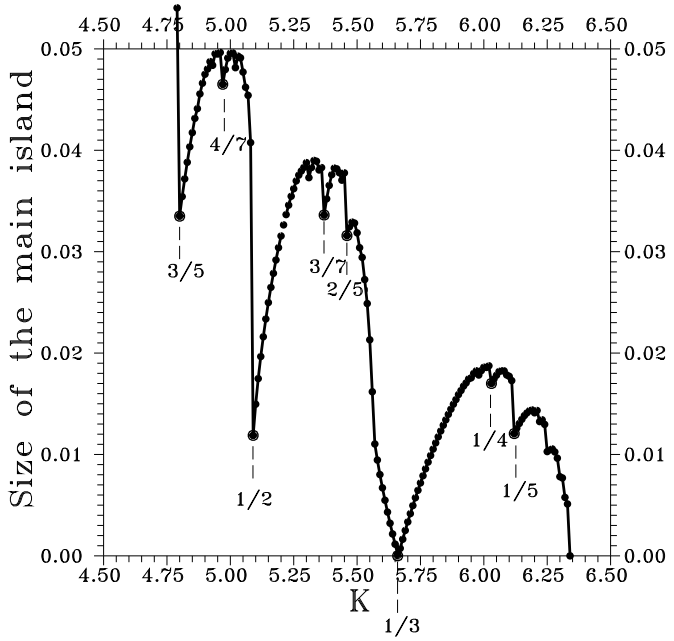

Figure 2. The size of the island (distance along the x-axis from the central periodic orbit to the last KAM curve on the left. We see the large variations of this distance whenever a last KAM curve is destroyed. The size of the island becomes zero at the bifurcation of the 1/3 resonance ($K \approx 5.66$) and for $K = 6.3345$ and beyond.

In figure 2 the size is measured along a line $y = y_p$ from the central periodic orbit (x_p, y_p) up to the last KAM curve (last KAM torus) to the left ($x < x_p$) surrounding the island, and we plot the value of $|x - x_p|$ as a function of K. Diagrams giving the approximate distance of the last KAM curve from the central periodic orbit were given by various authors (e.g. Schmidt and Bialek 1982).

According to Greene (1979) and Percival (1982) the last KAM invariant curve to be destroyed has a 'noble' rotation number. Namely the rotation number a, written as a continued fraction,

$$a = [a_1, a_2, \ldots] = \cfrac{1}{a_1 + \cfrac{1}{a_2 + \cdots}} \tag{5}$$

has a_i equal to 1 above a certain order ($i > N$).

The last KAM curve surrounding the five islands of figure 1 has rotation number equal to the 'golden number' $a = [1, 1, 1 \ldots]$ which is the simplest noble number. The successive truncations of this number are 1/2, 2/3, 3/5, 5/8, 8/13... and for each successive higher order truncation, they correspond to periodic orbits, which are alternatingly inside and outside the cantorus. For example, the periodic orbits 8/13 are inside the cantorus and closer to it than the periodic orbits 3/5. The orbits 2/3,5/8 are outside the cantorus, the second one being closer to the cantorus than the first.

The transition value K_c for the destruction of the torus $[1, 1, 1 \ldots]$ is close to $K = 4.79$.

For K larger than K_c the size of the island is limited by another last KAM curve, inside the 3/5 periodic orbits. As K increases, the size of this last KAM curve increases (figure 2). But when this size becomes maximum the new last KAM curve is also destroyed and the size

of the island decreases again (see the drops of the curve of figure 2 at the resonances 3/5, 4/7, 1/2, 3/7, 2/5, 1/3, 1/4, 1/5 etc).

Then another last KAM curve takes over and so on.

The curve of figure 2 has in fact infinite intervals where it increases on the average, with infinite abrupt decreases. In fact this curve is like the Weierstrass curve, which does not have a derivative at any point.

The increase in size of the islands is due to the pushing outwards of the various invariant curves with given rotation number. In fact, as K increases, new invariant curves are formed around the central periodic orbit with smaller and smaller rotation numbers.

When the rotation number goes through a rational number a new couple of periodic orbits (one stable and one unstable) bifurcates in general†.

This set moves outwards as K increases further and comes near the border of the island. Eventually the last KAM curve changes and comes inside this set of islands, that are now left in the large 'chaotic sea'.

In figure 2 we have marked the most important resonances, that produce large reductions of the size of the main island. We have not marked the higher order resonances that produce the secondary variations of the size of the main island.

In a previous paper (Efthymiopoulos *et al* 1997) we have examined the destruction of the noble KAM tori close to $a = [2, 1, 1 \ldots]$ in detail. There we had used counterclockwise rotation numbers which are complementary to our present clockwise rotation numbers. Therefore the previous $a = [2, 1, 1 \ldots]$ corresponds to our present $a = [1, 1, 1 \ldots] = 1 - [2, 1, 1 \ldots]$.

By comparing figures 11 and 12 of that paper, for $K = 4.791$ and 4.793 respectively, we see that the noble KAM curve $[2, 1, 1 \ldots]$ has been destroyed already for K between 4.79 and 4.791. But there are other KAM tori inside it for $K = 4.791$ namely $[2, 1, 1, 2, 1 \ldots]$, $[2, 1, 1, 3, 1 \ldots]$ and $[2, 1, 1, 4, 1 \ldots]$.

The noble torus $[2, 1, 1, 5, 1 \ldots]$ and other noble tori have been already destroyed.

Then for $K = 4.793$ the noble tori $[2, 1, 1, 2, 1 \ldots]$ and $[2, 1, 1, 4, 1 \ldots]$ are also destroyed, while the torus $[2, 1, 1, 3, 1 \ldots]$ still exists. Finally, for $K = 4.794$ this torus is also destroyed.

We conclude: (a) that the last KAM torus has not the simplest noble rotation number, and (b) the destruction of noble tori proceeds both from outside inwards and from inside outwards. The abrupt decrease of the size of the island occurs when not only the torus $[2, 1, 1, \ldots]$ but also the nearby tori are destroyed.

From now on we will again use clockwise rotation numbers. Figure 3 shows the form of the island for $K = 4.9$, near the maximum size of the last KAM curve with rotation number $a = [1, 1, 2, 1, \ldots]$. Inside this curve there are seven islands corresponding to the stable periodic orbit 4/7.

The islands 3/5 still exist, but they are much smaller than in figure 1, and they are embedded in the large 'chaotic sea'.

Similar processes occur around most transitions through the minima of the curve of figure 2.

In particular, a dramatic reduction of the size of the island, appears when the last KAM curve surrounding the two sets of islands of type 1/2 is destroyed (notice that in this case the four islands surround two different stable periodic orbits, each of type 1/2 ; there are also two unstable periodic orbits of type 1/2). The transition between figures 4 and 5 corresponds to points on both sides of the minimum of the curve of figure 2 near $K = 5.085$.

† Two couples of periodic orbits bifurcate in some cases (see figure 4).

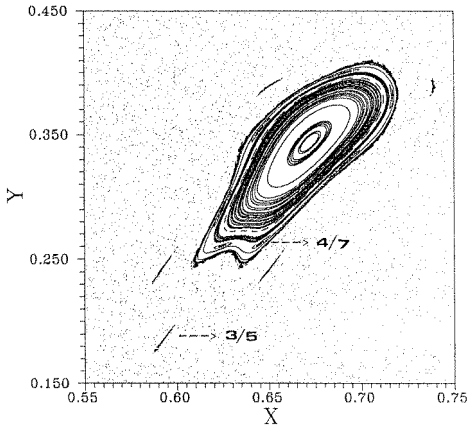

Figure 3. The main island for $K = 4.9$. The five islands of the orbit 3/5 are now in the 'chaotic sea', while the islands of the resonance 4/7 are inside the corresponding last KAM curve.

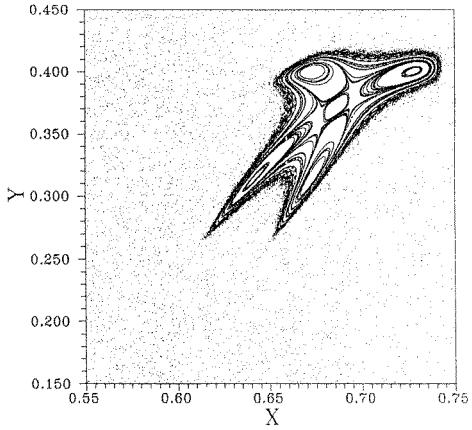

Figure 4. The main island for $K = 5.08$. It contains two sets of two islands corresponding to the resonance 1/2 inside the last KAM curve.

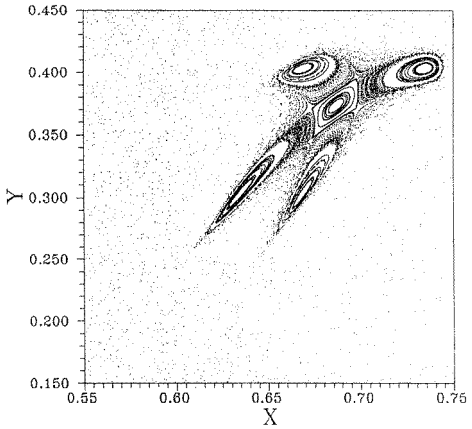

Figure 5. The main island for $K = 5.09$ is considerably smaller than in figure 5, while the two sets of two islands are now in the 'chaotic sea'.

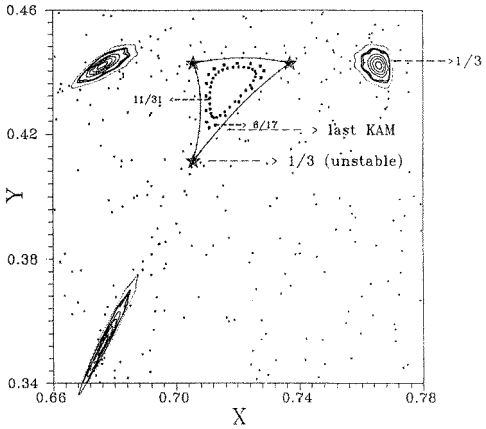

Figure 6. The main island for $K = 5.58$ is very small. It is limited by a triple unstable orbit, while a stable orbit 1/3 and a set of three islands is further away.

As K increases beyond 5.085 the size of the island increases and reaches a maximum near $|x - x_p| = 0.038$. But this is much smaller than the previous maximum, near $|x - x_p| = 0.05$, for K near 5.

Then we have one more drastic reduction of the size of the island, but not abrupt, as in the previous cases. This reduction leads to the vanishing of the island for $K \approx 5.66$.

As we approach this limiting case (figure 6 for $K = 5.58$) the size of the central island is reduced, while three secondary islands corresponding to the resonance 1/3 surround it. These islands are in the large 'chaotic sea'. The central island is limited by three unstable periodic orbits.

In figure 7 ($K = 5.74$) we see that the form of the island is different. The three unstable periodic orbits that limit the island now have a different orientation. In fact the vanishing of the central island occurs when the three unstable points of figure 6 move inwards and join at

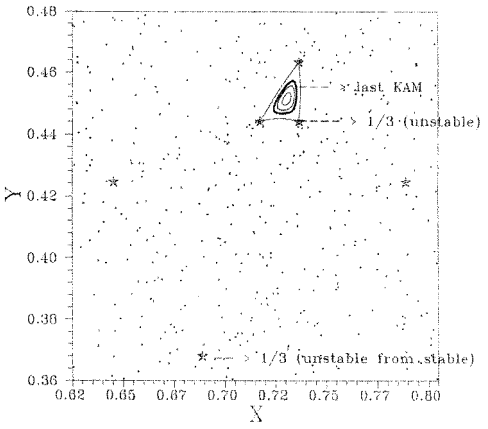

Figure 7. The main island for $K = 5.74$ is limited by a triple unstable orbit, but the position of this 1/3 orbit is different from that of figure 7. The stable 1/3 orbit has just become unstable.

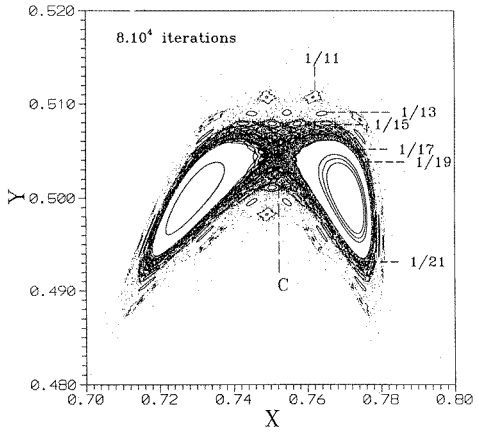

Figure 8. For $K = 6.34$ the central periodic orbit C is unstable. Two islands of stability on the left and on the right of C, have been produced by bifurcation from C. There is no island surrounding both islands, but only a sticky chaotic zone around C, and around both islands. This chaotic zone communicates with the outer large 'chaotic sea'. Some higher order islands are marked.

the centre. Then they are again separated, moving away from the centre as K increases. The outer islands have now become unstable.

Thus the central orbit is unstable only for one critical value of $K \approx 5.66$.

This phenomenon is well known (Contopoulos 1968). The triple periodic orbit, that bifurcates from the central orbit at the critical value of K, is unstable on both sides of the bifurcation.

For still larger K the size of the island reaches another maximum, near $|x - x_p| = 0.018$, much smaller than the previous maximum 0.038. Beyond that value of K the size of the island in general decreases until it becomes abruptly zero for $K = K_c = 6.3346$ and remains zero for larger K.

As we approach the limiting value $K = K_c$ the central periodic orbit becomes unstable by a period doubling bifurcation, generating two stable islands, on each side of it (figure 8, for $K = 6.34$). The bifurcation occurs at $K_b \approx 6.28$.

For a value of K smaller than K_b the central periodic orbit is surrounded by invariant curves and periodic orbits with rotation numbers small positive, but not reaching zero. For example, in figure 9 for $K = 6.28$ inside the last KAM curve we see islands with rotation number $\nu_\theta = 1/8, 1/9 \ldots$, up to 1/25 (in the cases of order 17 and higher only the periodic orbits are marked). This sequence reaches a minimum rotation number at the central periodic orbit (marked C in figure 9) which is slightly above zero. In the whole region inside the last KAM curve there is a little chaos around each unstable periodic orbit, but this is not conspicuous.

However, after the central periodic orbit C becomes unstable a chaotic domain develops around it and the sequence of invariant curves around C, terminates on the inner side at a certain distance from C, defined by a 'first' KAM curve between the first and the last KAM curves there are infinitely more KAM curves and infinitely higher-order islands. As K increases the first and the last KAM curves approach each other.

For $K = 6.334$ (figure 10) both the first and the last KAM curve are between the resonances 1/16 and 1/17, and for $K = 6.34$ (figure 8) all the KAM curves around C have been destroyed.

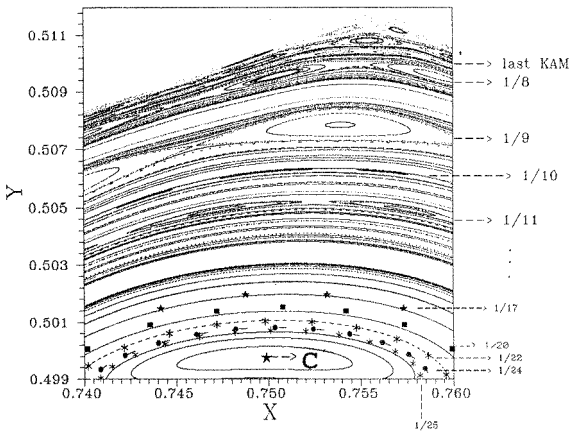

Figure 9. The region above the central periodic orbit C for $K = 6.28$. Then C is stable but close to instability. The point C is surrounded by a large set of invariant curves all the way from C to the 'last KAM curve'. This region contains many secondary islands of higher order.

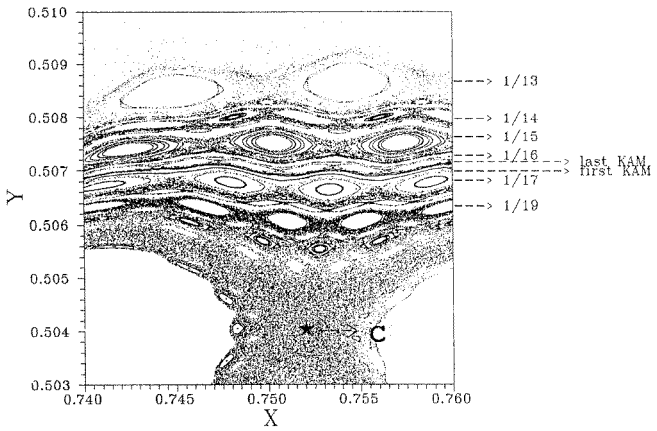

Figure 10. As figure 9 but for $K = 6.334$. Now the central periodic about C is unstable and is surrounded by a chaotic domain. Further to the left and to the right are two bifurcated islands. There are a 'first KAM curve' surrounding C and a 'last KAM curve'. These curves are very close to each other. For K a little larger they disappear altogether and we reach the case of figure 8.

The destroyed KAM curves have now become cantori. The most important cantori, i.e. those with the smallest holes, are in the region of the last KAM curves, i.e. near the resonance 1/16. When K is slightly above $K_c = 6.3346$ the chaotic domain around the unstable central periodic orbit C communicates with the outer 'chaotic sea', through the holes of these cantori. Orbits starting close to C stay for a long time in the inner chaotic domain before reaching the outer 'chaotic sea'. In figure 11 we give the 'stickiness time' (i.e. the time required for an orbit to go beyond a circle of radius 0.05 around C)as a function of the distance $\Delta y = y - y_c$ from the point C (x_c, y_c) upwards (for $x = x_c$). (If we change the radius around C the results change very little.) We see that in a region up to $\Delta y \approx 0.0035$ the stickiness time is roughly constant, of the order of $t = 10^6$ iterations on the average, but with large variations. We call this region the 'inner stickiness region'. The line $x = x_c$ passes through higher order islands, in which case there is no escape and the 'stickiness time' is infinite. The end of the inner stickiness region is roughly at the island 1/15. Beyond that the stickiness time decreases on the average outwards until it becomes quite small (figure 11).

Sometimes a point closer to C escapes faster than a point further away from C. This is

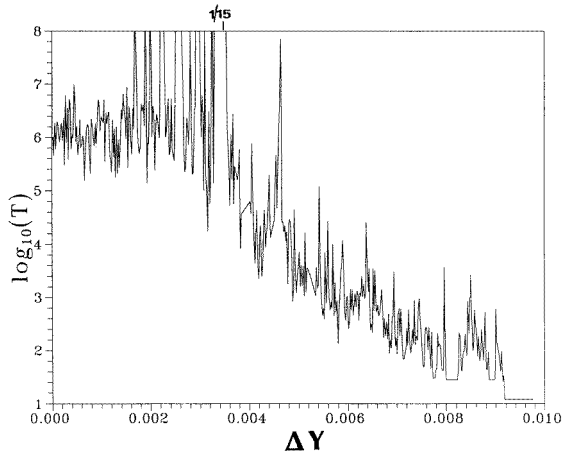

Figure 11. The stickiness time as a function of the distance $\Delta y = y - y_c$ upwards from the central periodic orbit C(x_c, y_c) for $K = 6.337$ and $x = x_C$.

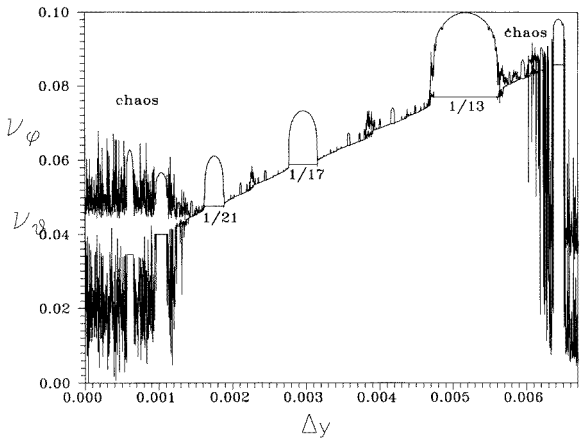

Figure 12. The curves ν_θ and ν_ϕ along a line $x = x_c$ from the central periodic orbit (x_c, y_c) upwards ($\Delta y = y - y_c$) and $K = 6.33$, with a step 10^{-5} in Δy. The orbits have been calculated for 10^5 iterations. The two curves coincide at invariant curves surrounding C. The secondary islands are represented by an inverse U in the ν_ϕ curve and by horizontal straight line segments in the ν_θ curve. The chaotic zones are represented by irregular variations of ν_θ and ν_ϕ.

explained by the fact that the escape route through the holes of the cantori is very complicated and the escape is not simply a diffusion outwards (Efthymiopoulos *et al* 1997).

When K increases the whole curve of figure 11 moves downwards, i.e. the stickiness time decreases in general.

We apply the method of the ROTOR, that we described earlier, along a line starting from the central periodic orbit upwards (i.e. for fixed x and increasing y). In figure 12 we show both curves ν_θ and ν_ϕ for $K = 6.33$. Close to the centre ($\Delta y = y - y_c \approx 0$) both curves ν_θ and ν_ϕ are very irregular, corresponding to the chaotic domain near C. Large irregularities also appear on the right of the figure, corresponding to the large 'chaotic sea' outside the island. Between these two chaotic regions the curves ν_θ and ν_ϕ coincide, except at the islands, where the curve ν_ϕ is of an inverse U shape, while the curve ν_θ has straight line segments. We see also some

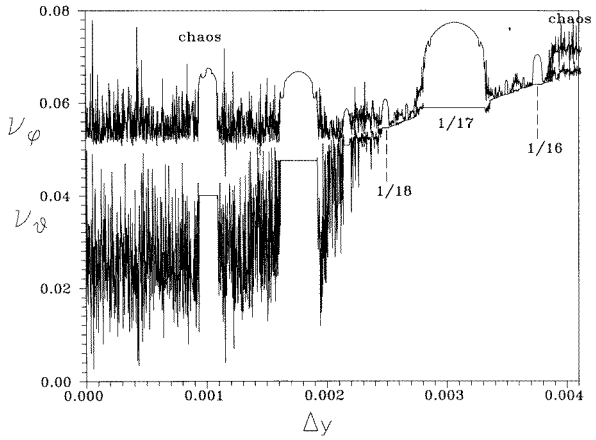

Figure 13. As figure 12 but for $K = 6.334$.

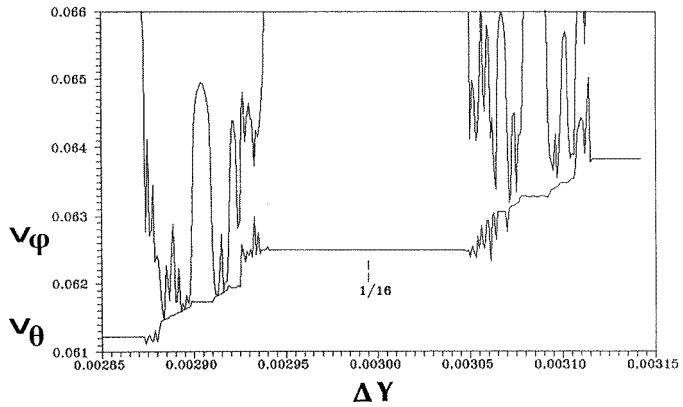

Figure 14. The curves ν_θ and ν_ϕ for $K = 6.3346$ in a small interval around the island 1/16. The step size of Δy is 10^{-6}. The orbits have been calculated for 10^6 iterations.

small secondary chaotic domains where both curves ν_ϕ and ν_θ are irregular. The islands in the chaotic domains are again characterized by inverse U shapes of the ν_ϕ curve and straight lines of the ν_θ curve.

The region of regular invariant curves extends from $\Delta y = 0.0014$ (first KAM curve) to $\Delta y = 0.0059$ (last KAM curve) and contains the islands from 1/13 to 1/21.

As K increases (figure 13 for $K = 6.334$) the ordered region decreases. Now only the main secondary islands 1/16 and 1/17 and some high-order islands are in the ordered domain.

For $K = 6.3346$ (figure 14) we have found the details of the curves ν_θ and ν_ϕ around the island 1/16. By calculating the orbits for larger times (10^6 iterations) and with a smaller step size in Δy (10^{-6}). We see that the two curves continue to touch each other on the left of the island 1/16, but they have been disconnected on the right of 1/16. Thus there are no KAM curves on the right of the island 1/16. This has been verified by calculating an orbit close to the island 1/16, which diffused outwards, reaching the large 'chaotic sea'.

Thus, in order to check whether the curves ν_θ and ν_ϕ coincide, or only come close to each other, one has to calculate ν_θ and ν_ϕ more accurately, i.e. for longer times with a smaller time

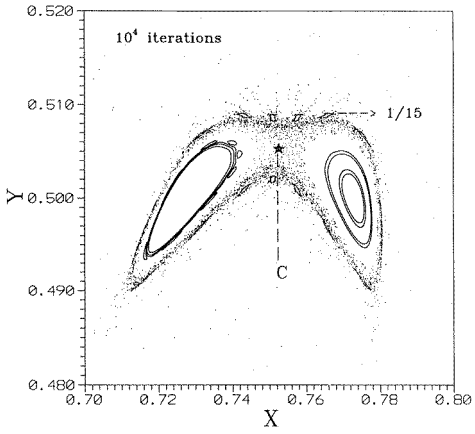

Figure 15. A sticky zone close to the island 1/16 surrounding the point C for $K = 6.35$. In this case there are no 'first'and 'last' KAM curves around C, but there is still a sticky ring around C and around both islands on the left and of the right of C.

step size. But we can only be certain that the last KAM curve in an interval has been destroyed by finding an orbit that passes from one side of this interval to the other. For further details see the recent paper of Voglis *et al* (1998). If we change the line (from C) along which we measure the frequencies ν_θ and ν_ϕ, the figures 12–14 change, but they remain qualitatively similar. Namely the sequence of resonances is the same, although some islands may disappear if the line passes through the chaotic domain close to an unstable periodic orbit between islands of the same order. Furthermore, the new line crosses the same KAM curves and at these points the values ν_θ and ν_ϕ coincide.

From figures 12–14 it follows, by extrapolation, that the first and last KAM curves coincide and disappear at the critical value $K = K_c$ slightly larger than 6.3346. This is what is usually called the 'last KAM curve' that separates (for smaller K) and joins (for larger K) two chaotic domains. This last KAM curve has a noble rotation number.

We remark here, as in previous cases (Efthymiopoulos *et al* 1997), that this is not the simplest noble number, as one would expect by applying the conjecture of Greene (1979) for the destruction of the last KAM curve.

For K larger than K_c there are no closed invariant curves around C. If we construct diagrams like figures 12–14 we see that the curves ν_θ and ν_ϕ never coincide. However, orbits starting near C spend a long time in the neighbourhood of the island 1/16 before escaping to the large 'chaotic sea'. Thus a sticky zone remains in this region, which becomes less and less prominent as K increases (cf figure 8 for $K = 6.34$ with figure 15 for $K = 6.35$).

On the sides of the central point C the two islands generated by bifurcation from C, when C becomes unstable, still exist for even larger K. But the periodic orbits at the centres of these islands also become unstable, by another period doubling bifurcation, and finally, after an infinity of further period doubling bifurcations, all the periodic orbits produced from C, directly or indirectly, become unstable. Thus all the islands in this region disappear. For even larger K only small islands, independent of those generated by a cascade of periodic doubling bifurcations from C, still remain. But their study is beyond the scope of this paper.

3. Evolution of the main island of the Hamiltonian (2)

We consider the evolution of the main island of the Hamiltonian (2) for $\omega_1^2 = 1.6$, $\omega_2^2 = 0.9$, $h = 0.007\,65$, while ϵ is the nonlinearity parameter that varies from one case to another. This evolution is very similar to that of the case of the map (1).

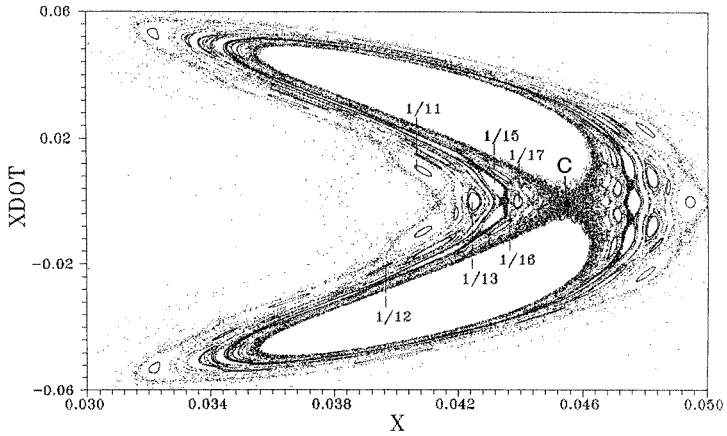

Figure 16. A Poincaré surface of section around the central unstable periodic orbit C of the Hamiltonian (2) for $\epsilon = 4.41$. Some islands $(1/11, 1/13, 1/15, 1/17)$ are marked.

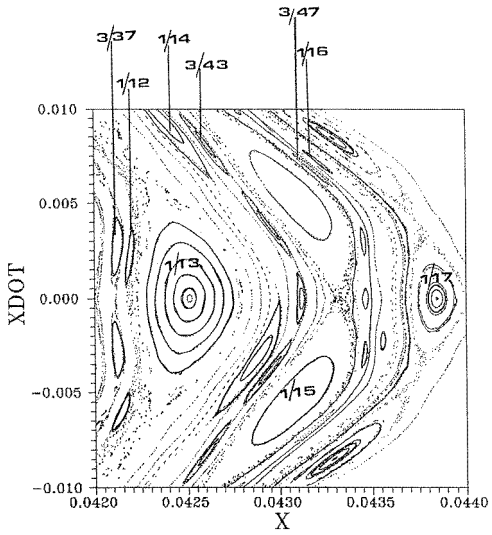

Figure 17. Part of the Poincaré surface of section for $\epsilon = 4.405$.

In the Hamiltonian cases we have used a fourth-order Runge–Kutta routine. As our discussion is mainly qualitative no greater accuracy was needed. For example, the energy was conserved with eight significant figures. The periodic orbits were located by a Newton–Raphson algorithm.

For relatively small ϵ ($\epsilon \leqslant 4.306$) the central periodic orbit is stable and is surrounded by a large set of invariant curves and periodic orbits. The distribution of periodic orbits for various values of ϵ has been studied by Contopoulos *et al* (1996).

The central periodic orbit C becomes unstable for $\epsilon = 4.3061$, and as ϵ increases, all the periodic orbits recede from C, while a chaotic domain develops around C. At the transition to instability a bifurcation of two stable period-1 orbits takes place. These orbits are above and below C, and they are surrounded by two islands of stability (figure 16).

The central chaotic domain increases with ϵ and the two islands of stability increase in size. At the same time the outer 'chaotic sea', that surrounds both these islands, increases inwards.

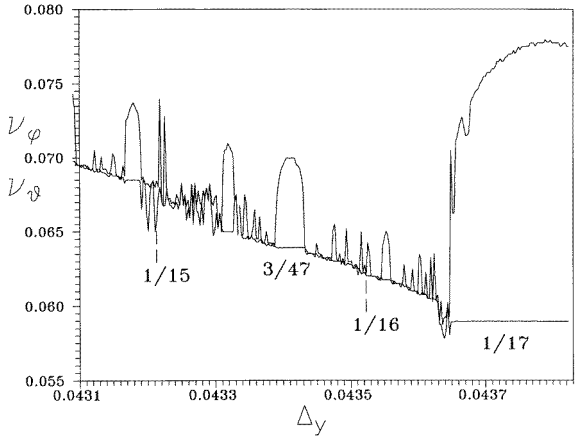

Figure 18. The values of ν_θ and ν_ϕ as functions of x after $N = 10^4$ iterations in the case $\epsilon = 4.405$ (cf figure 17).

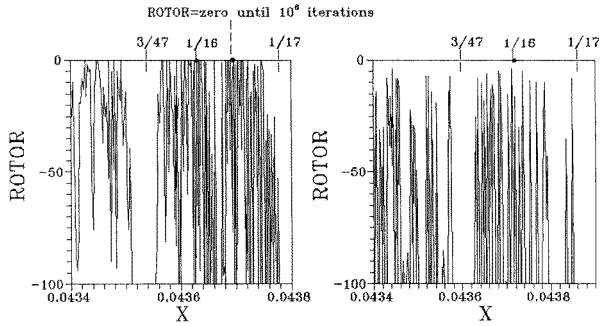

Figure 19. The ROTOR = $\nu_\theta - \nu_\phi$ as a function of x in the cases (a) $\epsilon = 4.41$ and (b) $\epsilon = 4.415$, for $N = 2 \times 10^4$ iterations. In case (a) we mark also the points where the ROTOR remains zero after $N = 10^6$ iterations (in all other points the ROTOR is negative).

However, the outer and inner chaos do not communicate for $\epsilon < 4.41$. For $\epsilon = 4.405$ there are closed invariant curves (KAM curves) surrounding C and the two islands above and below it. In figure 17 we give the detailed structure of the islands in the region between 3/37 and 1/17 for $\epsilon = 4.405$. The closed invariant curves are between the resonances 1/15 and 1/17.

A proof that there are in fact closed KAM curves in these regions is provided by the diagrams of ν_θ and ν_ϕ (figure 18, for $\epsilon = 4.405$) as in the case of the standard map (figures 12–14). We see that the curves ν_θ and ν_ϕ coincide, for $N = 10^4$ iterations, in some intervals between the resonances 1/15 and 1/16 and also between 1/16 and 1/17. The reality of these coincidences is verified by longer calculations ($N = 10^5$). In contrast the coincidences between 3/43 and 1/15 in figure 18 are not real, because the longer calculations show that the lines ν_θ and ν_ϕ are not reaching each other in this region.

We also calculated the values of ν_θ and ν_ϕ in the cases $\epsilon = 4.41$ and $\epsilon = 4.415$. As the lines of ν_θ and ν_ϕ are quite complicated, we give in figures 19(a) and (b) only the difference $\nu_\theta - \nu_\phi$ as a function of x.

In the case $\epsilon = 4.41$ (figure 19(a)) we see that if the number of iterations is $N = 2 \times 10^4$ there seem to be many values of x for which the ROTOR is zero. However, if N becomes larger

($N = 10^6$) only for two values of x does the ROTOR remains zero. On the other hand for $\epsilon = 4.415$ and $N = 2 \times 10^4$ the ROTOR does not become zero between the resonances 1/16 and 1/17 (figure 19(*b*)), therefore the inner and outer chaos communicate. There is only some delay in this communication, due to the cantori that exist in the region between the resonances 1/15 and 1/17.

Therefore, the destruction of the invariant curves surrounding the central point C occurs for ϵ slightly larger than $\epsilon = 4.41$. The last KAM curves appear between the resonances 1/16 and 1/17 (figure 17). We conclude that the destruction of the invariant curves around C in that case of the Hamiltonian (2) follows a similar pattern as in the case of the map (1).

4. Evolution of the main island of the Hamiltonian (3)

A different pattern of creation of chaos is when the central orbit becomes unstable by an 'inverse' (subcritical) bifurcation (Contopoulos 1983a).

In this case the bifurcating family is unstable and exists for parameter values for which the central orbit is stable.

Such cases appear in the Hamiltonian (3) (Contopoulos *et al* 1994) for a fixed value of the energy ($h = 1$). In this case the cental periodic orbit has an infinity of transitions from stability to instability and vice versa, as the perturbation ϵ increases to infinity. If ϵ is positive there is never any escape to infinity. The value of h is equal to unity.

Whenever we have a transition from stability to instability for increasing ϵ, there is a bifurcation of equal period periodic orbits, which is direct, i.e. the bifurcating family is stable and exists for values ϵ larger than the bifurcation value ϵ_B, while the central family is unstable for ϵ larger than ϵ_B (but not very large). For example, this occurs when ϵ goes beyond $\epsilon_B = 1.457$. Similar direct bifurcations appear for $\epsilon_B = 4.131$, $\epsilon_B = 8.098$ etc. In all these cases the bifurcation scenario is the same as in the case of the map (1) and the Hamiltonian (2). When the central periodic orbit ($y = \dot{y} = 0$) becomes unstable a chaotic domain develops around it, which grows larger as ϵ increases. At the same time a large 'chaotic sea', outside the island, grows inwards and beyond a certain value of $\epsilon = \epsilon_c > \epsilon_B$ the inner and outer chaos join and destroy the central island. Only two secondary islands remain above and below the centre (i.e. for $y = 0$, and $\dot{y} > 0$ and symmetrically for $\dot{y} < 0$; figure 4 of Contopoulos *et al* 1994).

The situation is different at a bifurcation from instability to stability, e.g. for $\epsilon'_B = 2.154$. Then the central orbit O becomes again stable and for $\epsilon > \epsilon'_B$ two unstable orbits of equal period appear for $\dot{y} = 0$, $y > 0$ (O_2) and a symmetric point $y < 0$ (O_1, figure 20).

In order to study the destruction of the island of stability around the centre it is best to consider ϵ decreasing through the value ϵ_B. As ϵ decreases the island around O decreases in size but no chaotic domain appears around O. In fact there are only some higher order periodic orbits inside the island, forming rings of stable and unstable points, and small chaotic zones appear around the unstable points. This phenomenon is so general that it does not require a detailed description here.

The inner asymptotic curves from O_1 and O_2, that limit the island around O, produce extremely small regions of chaos near the borders of the island, while the outer asymptotic curves produce a large chaotic domain (figure 20, for $\epsilon = 2.5$). However the inner chaotic zone communicates with the outer chaos.

A remark concerning the nomenclature is in order here. The asymptotic curves of the orbits O_1 and O_2, intersect at heteroclinic points, like H and H'. However when ϵ decreases below ϵ_B the points O_1 and O_2 merge at the centre O, and the points of intersection of the asymptotic curves are called homoclinic points.

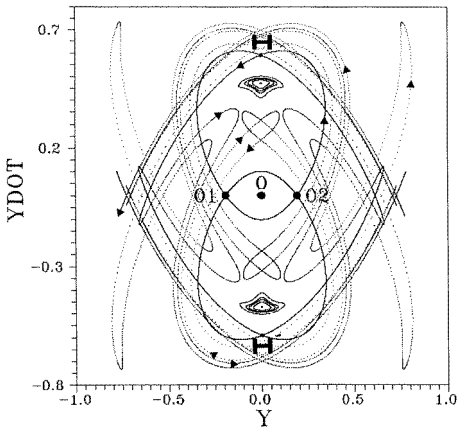

Figure 20. The asymptotic curves from the unstable periodic orbits O_1 and O_2 in the Hamiltonian (3) for $\epsilon = 2.5$ and $h = 1$. The outer asymptotic curves intersect at many heteroclinic points like H and H'. The arrows follow an outer unstable asymptotic curve from O_2. The inner asymptotic curves surround the stable periodic orbit O and the central island around it.

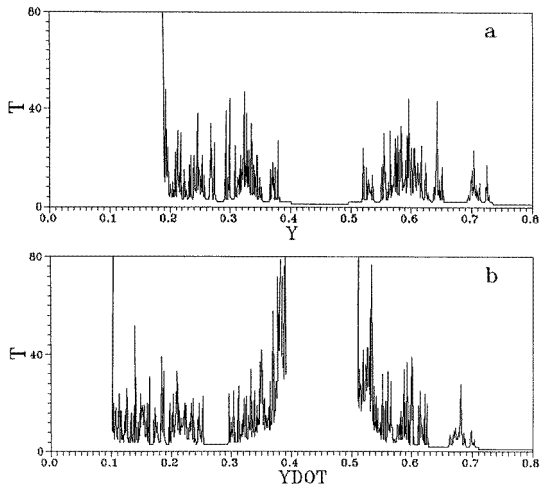

Figure 21. The stickiness time T: (*a*) as a function of y along the y-axis, and (*b*) as a function of $\dot{y}$ along the $\dot{y}$-axis, for $\epsilon = 2.5$.

In order to find the stickiness around the central island in the case $\epsilon = 2.5$ we calculate, first, the time required by various orbits to cross a circle of radius 0.8 around the centre and we call it the 'stickiness time'. A change in this radius does not change our results appreciably.

In figure 21 we show the stickiness time T as a function of y and $\dot{y}$. The stickiness time is infinite inside the central island and inside a large island above it (figure 21(*b*)). Between these two islands the stickiness time is on the average constant ($T \approx 10$), but with large variations. Close to the second island, T increases considerably and beyond it decreases again, and reaches very small values beyond $\dot{y} = 0.71$.

Along the y-axis the stickiness beyond O_2 at the end of the main island ($y \approx 0.2$) has again an average value $T \approx 10$, with large variations, and reaches very small values beyond $y = 0.73$ (figure 21(*a*)). If we change the direction along which we measure the stickiness times we find figures qualitatively similar to figures 21(*a*) and (*b*).

In both figures 21(*a*) and (*b*) there are some flat regions with very small values of T (especially between $y = 0.4$ and $y = 0.5$). These are the regions of fast escape through openings of the stable asymptotic curves (Efthymiopoulos *et al* 1997).

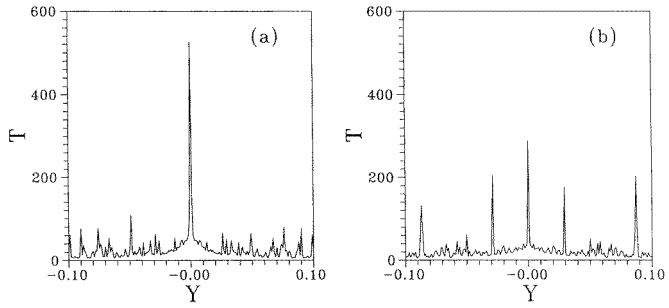

Figure 22. The stickiness time T as a function of y along the y-axis for (a) $\epsilon = 2.153$ and (b) $\epsilon = 2.150$. In both cases the central orbit O is unstable.

As ϵ decreases O_1 and O_2 approach each other and the inner asymptotic curves tend to a separatrix, but the size of these curves tends to zero, as the whole island around O tends to zero. The periodic orbit O becomes unstable as ϵ decreases below $\epsilon'_B = 2.154$ and the stickiness around it is small.

The stickiness in the case of inverse bifurcations is not due to cantori surrounding the central island. Such cantori should exist for smaller values of ϵ ($0 < \epsilon < \epsilon_B = 1.457$), when the central orbit is stable, and for ϵ somewhat larger than ϵ_B (as in figures 8 and 15). However, for values of ϵ as large as $\epsilon = 2.1$, or larger, these cantori move far away from the centre O. They have large gaps and thus they do not produce appreciable stickiness around them. The stickiness near the boundaries of the main island is due mainly to the usual delay of escape of the iterates of an orbit in the neighbourhood of the unstable periodic orbits O_1 and O_2 from these orbits and from their asymptotic curves, if the unstable eigenvalues of these orbits are not much larger than 1 (figure 21). In our examples any cantori between the unstable orbits O_1 and O_2 are congested in a very small region near the boundary of the island.

This kind of stickiness also appears for $\epsilon < \epsilon'_B$, when the central orbit O is unstable. In figure 22 we give the stickiness time T as a function of y for two values of ϵ, smaller than but close to ϵ'_B, namely (a) $\epsilon = 2.153$ and (b) $\epsilon = 2.150$. In both cases T is maximum near the centre and decreases outwards. The central maximum is larger in the first case, which is very close to the critical value $\epsilon'_B = 2.154$. In this case the eigenvalue of the unstable orbit O is close to 1, while it is much larger in the second case. As a consequence the stickiness near O is larger in the first case than in the second. However, if we reduce ϵ still further and approach the critical value $\epsilon_B = 1.457$ we have again larger stickiness, due to cantori (as we described in the previous section).

Similar results appear at other transitions from stability to instability, as ϵ decreases through higher order critical values, like $\epsilon_B = 5.506$, $\epsilon_B = 10.100$ etc.

5. The evolution of a major island in the Sitnikov problem

A similar phenomenon of an abrupt disappearance of an island by the merging of two outer unstable orbits, without having first a transition to instability of the central periodic orbit, appears in the Sitnikov problem (Sitnikov 1960).

The Sitnikov problem refers to the motion along the z-axis of an infinitesimal particle, moving in the field of two equal masses (primaries) that describe ellipses around their common centre of mass (origin in the x, y plane) with eccentricity e.

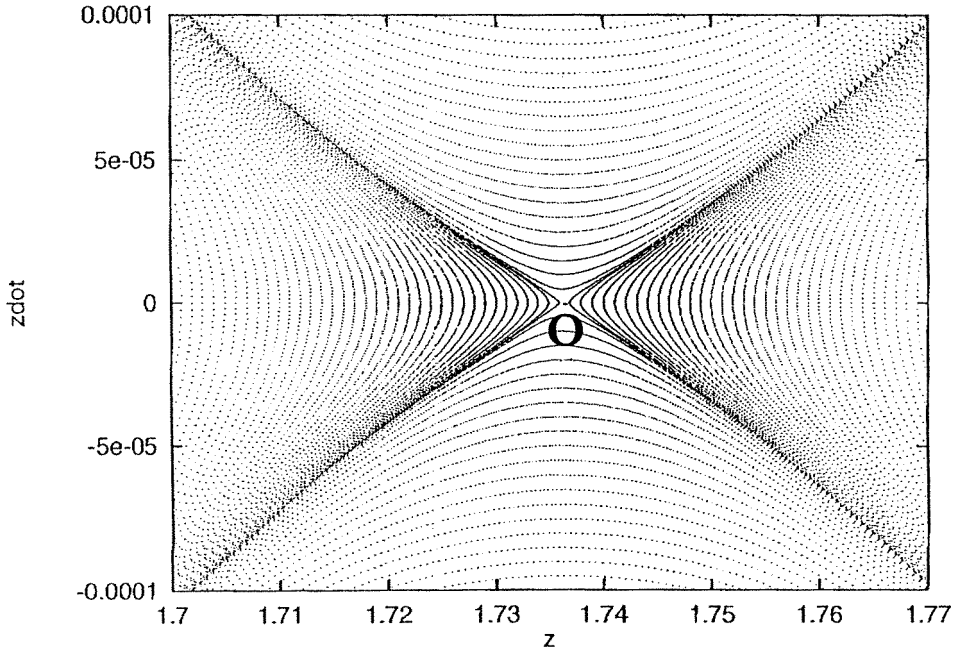

Figure 23. The Poincaré surface of section $(z, \dot{z})$ around the unstable point O for $e = 0.847$.

The equation of motion is

$$\ddot{z} + (r^2 + z^2)^{-3/2} z = 0 \tag{6}$$

where z is the distance of the massless body from the barycentre of the primaries and $r = r(t)$ is the distance of the primaries from the barycentre, which is found by solving the Kepler problem and is a known function of time t.

There exist many theoretical studies concerning the Sitnikov problem (e.g. Moser 1973, Liu and Sun 1990, Wodnar 1991 and 1993, Hagel 1992) and also numerical experiments where Poincaré surfaces of section for different values of the eccentricity of the primaries were constructed (e.g. Dvorak 1993). In another numerical investigation the stability and the stickiness around the central fixed point at $z = \dot{z} = 0$ was studied and is described in detail in Dvorak (1998). This orbit has many transitions from stability to instability and vice versa when e approaches 1 (Alfaro and Chiralt 1993).

In this paper we explore the stickiness around a resonant periodic orbit 2:1, when this orbit becomes unstable, by an inverse bifurcation, as e decreases through a critical value $e' = 0.847$. We consider a Poincaré surface of section giving the values of z and $\dot{z}$ when the primaries are at pericentre. This orbit is represented by two symmetric points $(+z, -z, \dot{z} = 0)$ on the z-axis.

The 2:1 orbit exists for all values of e. For small $e > 0$ it is stable and each point is surrounded by an island of stability, which is inside the 'mainland' of closed invariant curves around the centre. Beyond $e \approx 0.04$ this stable island is separated from the 'mainland' and the chaotic region around the island joins the chaotic regions outside and thus escapes are possible.

For larger eccentricities $e > e_B = 0.55$ the 2:1 orbit becomes unstable by a direct bifurcation generating stable 4:1 islands, that exist for e somewhat larger than e_B.

For even larger $e = e'_B = 0.847$ the 2:1 orbit (O) becomes again stable by an inverse bifurcation. The periodic orbit O is unstable for $e < e'_B$ (figure 23) and stable for $e > e'_B$

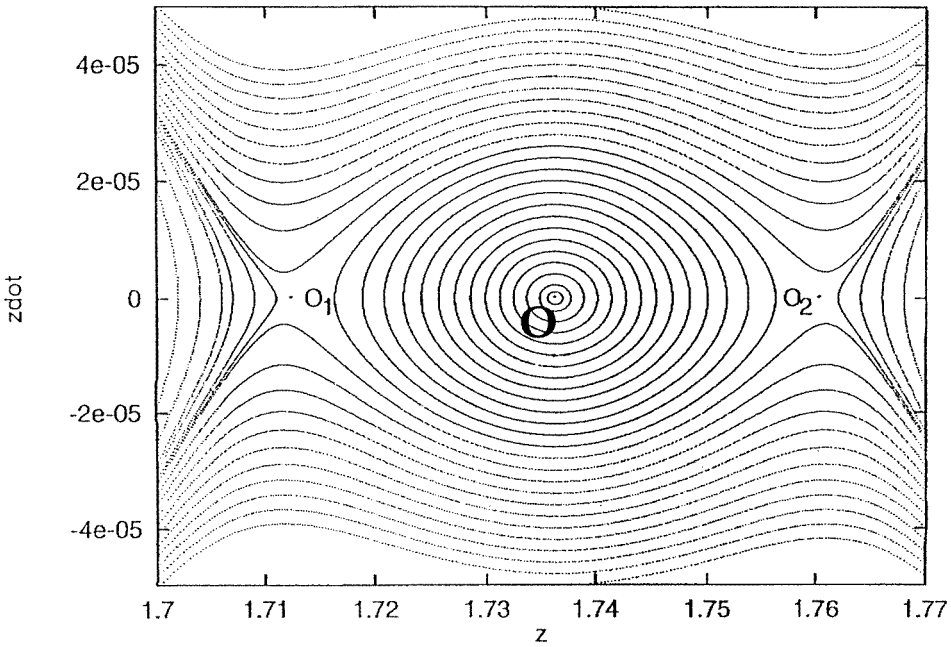

Figure 24. The Poincaré surface of section $(z, \dot{z})$ around the stable point O for $e = 0.8471$.There are two unstable points $O_1$and O_2 on the left and on the right of O.

(figure 24). In the second case O is surrounded by an island of stability which is limited by two unstable orbits O_1 and O_2 on the z-axis. The situation is very similar to the case of the Hamiltonian (3) studied above (figure 20) except in one important way: in the present case the orbits can escape to infinity, while in the Hamiltonian (3) there are no escapes. In particular, the asymptotic curves of the orbit O in figure 23 extend to infinity.

Similarly, the outer asymptotic curves of the orbits O_1 and O_2 of figure 24 extend to infinity. However, the inner asymptotic curves (left from O_2 and right from O_1), intersect each other at infinite points and generate a very thin chaotic layer close to the border of the island.

Inside the island surrounding O there are higher order stable and unstable periodic orbits and thin chaotic layers that we cannot see in figure 24.

In figure 25 we give the stickiness time T around the point O, defined as the time required by an orbit starting at $(z, \dot{z} = 0)$ to go beyond a circle of radius 3.0 around the barycentre. (If we change this radius the results do not change appreciably.) The stickiness time is given in three cases: $e_1 = 0.848 > e'_B$, $e_2 = 0.846 < e'_B$ and $e_3 = 0.84$. In the first case the stickiness time goes to infinity at the borders of the island. Somewhat away from the island on the left and on the right of figure 25 the stickiness curve is approximately a straight line. In these regions the stickiness time increases exponentially as the distance from the island decreases. However, very close to the island, the increase of T is superexponential. This phenomenon is generic and it has been observed in various dynamical systems (e.g. Contopoulos *et al* 1997).

As e decreases below e'_B (second case) the orbit O is unstable, but when e is close to e'_B the eigenvalue of O is only slightly larger than 1, and the escape from the neighbourhood of O is slow (case $e = e_2 = 0.846$).

When e becomes smaller the eigenvalue of O is larger and the escape from the neighbourhood of O is faster. Thus the whole stickiness curve for $e = 0.84$ is lower than

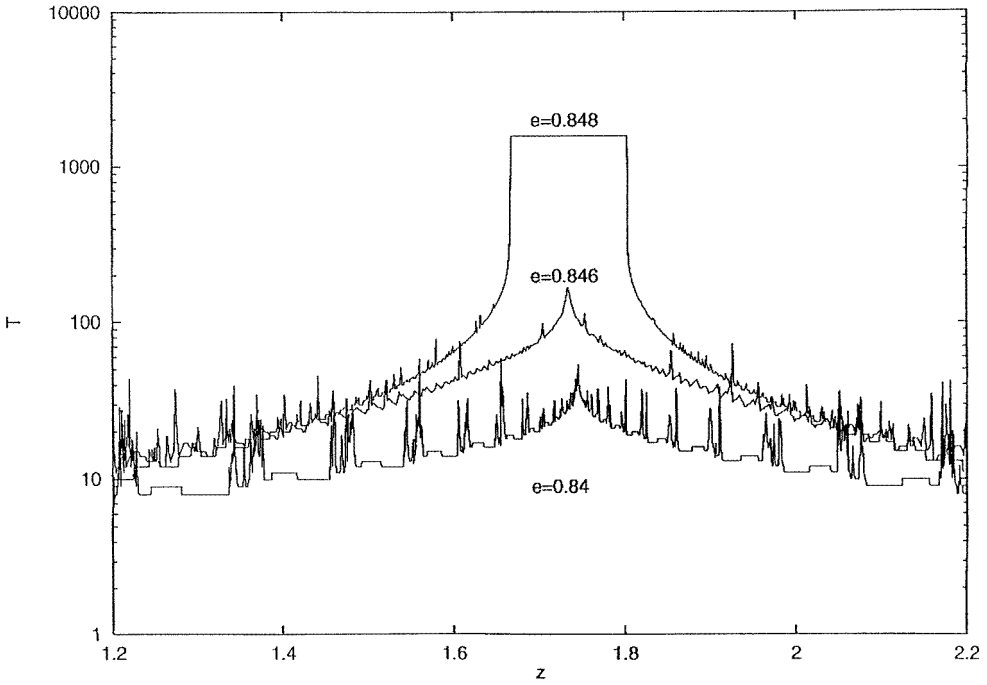

Figure 25. The stickiness time T as a function of the initial distance z of an orbit for $\dot{z} = 0$.

for $e = 0.846$.

This behaviour is similar to that of the Hamiltonian (3) (figures 21 and 22) but in the present case the noise in the stickiness curves is much smaller.

6. Conclusions

(1) We have found two basic types of stickiness (a) for direct (supercritical) pitchfork bifurcations and (b) for inverse (subcritical) bifurcations. (a) In direct bifurcations there is stickiness near the boundary of a stable island surrounding a periodic orbit at the centre of the island. When this orbit becomes unstable, as the perturbation increases, it develops a chaotic domain around it, but for a certain interval of values of the perturbation this chaotic domain does not communicate with the outer 'chaotic sea'. For a larger perturbation the KAM curves surrounding the central orbit are destroyed and become cantori with small gaps. Then the inner and the outer chaotic domains communicate but there is still stickiness for appreciable times. (b) In inverse bifurcations the stickiness is due mainly to the difficulty of escape from the neighbourhood of an unstable periodic orbit when its eigenvalue is not large. In this case an island of stability is limited by two unstable periodic orbits, that generate stickiness around them. When the perturbation decreases the island shrinks and disappears and the central orbit becomes unstable. Then there is stickiness around this orbit. In this case there are no cantori with small gaps.

(2) Our results seems to be generic, i.e. they are qualitatively similar in quite different problems. We have considered stickiness in direct bifurcations of the standard map and of a Hamiltonian with a cubic nonlinearity, and inverse bifurcations in a Hamiltonian with a quartic nonlinearity and in the Sitnikov problem. The last two problems also have direct

bifurcations, where the first type of stickiness is clearly seen.

(3) In our problems we have found direct bifurcations when the perturbation increases and inverse bifurcations when the perturbation decreases. However, in other problems the opposite is true. Thus the important distinction is not whether the perturbation increases or decreases, but whether a bifurcation is direct or inverse.

(4) Finally there are some quantitative differences in the stickiness time for cases with escapes but not as regards the main qualitative properties of direct and inverse bifurcations.

Acknowledgment

This research was supported in part by the Research Committee of the Academy of Athens (grant 200/437).

References

Alfaro J M and Chiralt C 1993 *Cel. Mech. Dyn. Astron.* **55** 351
Argyris J, Faust G and Haaze M 1994 *An Exploration of Chaos* (Amsterdam: North-Holland)
Aubry S 1978 *Solitons and Condensed Matter Physics* ed A R Bishop and T Schneider (Berlin: Springer) p 264
Chirikov B V and Shepelyansky D L 1984 *Physica* D **13** 395
Contopoulos G 1968 *Astrophys. J.* **153** 83
——1970 *Astron. J.* **75** 108
——1971 *Astron. J.* **76** 147
——1983a *Lett. Nuovo Cimento* **38** 257
——1983b *Physica* D **8** 142
Contopoulos G, Grousousakou E and Polymilis C 1996 *Cel. Mech. Dyn. Astron.* **64** 363
Contopoulos G, Papadaki H and Polymilis C 1994 *Cel. Mech. Dyn. Astron.* **60** 249
Contopoulos G, Voglis N, Efthymiopoulos C, Froeschlé C, Gonczi R, Lega E, Dvorak R and Lohinger E 1997 *Cel. Mech. Dyn. Astron.* **67** 293
Dana I and Fishman S 1985 *Physica* D **17** 63
Dvorak R 1993 *Cel. Mech. Dyn. Astron.* **56** 71
——1998 *The Dynamics of Small Bodies in the Solar System. A Major Key to Solar System Studies* ed A E Roy (Dordrecht: Kluwer Academic) p 509
Efthymiopoulos C, Contopoulos G, Voglis N and Dvorak R 1997 *J. Phys. A: Math. Gen.* **30** 8167
Greene J M 1979 *J. Math. Phys.* **20** 1183
Hagel J 1992 *Cel. Mech. Dyn. Astron.* **53** 267
Hénon M 1965 *Ann. Astrophys.* **28** 992
Liu J and Sun Y-S 1990 *Cel. Mech. Dyn. Astron.* **49** 285
Meiss J D and Ott E 1986 *Physica* D **20** 387
Moser J 1973 *Random and Stable Motion in Dynamical Systems* (Princeton, NJ: Princeton University Press)
Percival I C 1979 *Nonlinear Dynamics and the Beam–Beam Interaction* ed M Month and J C Herrera (Woodbury, NY: AIP) p 302
——1982 *Physica* D **6** 67
Schmidt G and Bialek J 1982 *Physica* D **5** 397
Shirts R B and Reinhardt W D 1982 *J. Chem. Phys.* **77** 5204
Sitnikov K 1960 *Dokl. Akad. Nauk., USSR* **133** 303
Voglis N, Contopoulos G and Efthymiopoulos C 1998 *IAU Colloquium* **172** at press
Voglis N and Efthymiopoulos C 1998 *J. Phys. A: Math. Gen.* **31** 2913
Wodnar K 1991 ed A E Roy (*Predictability, Stability and Chaos in N-body Dynamical Systems* (New York: Plenum)
——1993 *Cel. Mech. Dyn. Astron.* **56** 99